

IHEP 2008-27

OEF

Observation of the destructive interference in  
the radiative kaon decay  $K^- \rightarrow \mu^- \bar{\nu} \gamma$

O.G. Tchikilev, S.A. Akimenko, G.I. Britvich, A.P. Filin,  
A.S. Konstantinov, I.Y. Korolkov, V.M. Leontiev, V.F. Obraztsov,  
V.A. Polyakov, V.I. Romanovsky, V.K. Semenov, V.A. Uvarov,  
O.P. Yushchenko

*Institute for High Energy Physics, Protvino, Russia*

V.N. Bolotov, V.A. Duk, A.I. Makarov, A.A. Khudiakov, V.P. Novikov,  
A.Yu. Polyarush

*Institute for Nuclear Research, Moscow, Russia*

## Abstract

Using data collected with the “ISTRA+” spectrometer at U70 proton synchrotron of IHEP, we report the first measurement of the destructive interference in the radiative kaon decay  $K^- \rightarrow \mu^- \bar{\nu} \gamma$ . We find the difference of the vector and axial form factors  $F_V - F_A = 0.126 \pm 0.027(\text{stat}) \pm 0.043(\text{syst})$ . The measured value is two standard deviations above the  $O(p^4)$  ChPT prediction equal to 0.055. Inclusion of exotic tensor interaction gives  $F_V - F_A = 0.144 \pm 0.044(\text{stat}) \pm 0.035(\text{syst})$  and  $F_T = -0.0079 \pm 0.0113(\text{stat}) \pm 0.0073(\text{syst})$ , i.e.  $-0.03 < F_T < 0.01$  at 90% CL, consistent both with zero and with recent theoretical prediction equal to  $|F_T| = 0.022$ .

## 1 Introduction

The decay  $K^- \rightarrow \mu^- \bar{\nu} \gamma$  proceeds via two distinct mechanisms: the internal Bremsstrahlung (IB) with the photon emitted by the kaon or the muon, and the structure-dependent(SD) decay involving emission of the photon from intermediate states. SD is sensitive to the electroweak structure of the kaon and allows for good test of theories describing hadron interactions and decays, like Chiral Perturbation Theory (ChPT)[1, 2]. This decay is also a good place for searches for possible tensor interactions, see theoretical [3, 4, 5, 6, 7] and experimental [8, 9, 10, 11] papers, devoted mainly to the  $\pi \rightarrow e \nu \gamma$  decay. The differential probability of the decay can be written in terms of  $x = \frac{2E_\gamma}{M_K}$  and  $y = \frac{2E_\mu}{M_K}$  (where  $M_K$  is the kaon mass and  $E_\gamma$  and  $E_\mu$  are the photon and muon energies in the kaon rest frame). In the most general case, which includes hypothetical tensor term it reads:

$$\begin{aligned} \frac{d\Gamma}{dx dy} = & A_{IB} f_{IB}(x, y) + A_{SD} [(F_V + F_A)^2 f_{SD+}(x, y) + (F_V - F_A)^2 f_{SD-}(x, y)] \\ & - A_{INT} [(F_V + F_A) f_{INT+}(x, y) + (F_V - F_A) f_{INT-}(x, y)] + A_T F_T^2 f_T(x, y) \\ & - A_{IBT} F_T f_{IBT}(x, y) - A_{SDT} F_T (F_V - F_A) f_{SDT}(x, y). \end{aligned}$$

$$f_{IB}(x, y) = \left[ \frac{1 - y + r}{x^2(x + y - 1 - r)} \right] \left[ x^2 + 2(1 - x)(1 - r) - \frac{2xr(1 - r)}{x + y - 1 - r} \right], \quad (1)$$

$$f_{SD+}(x, y) = [x + y - 1 - r][(x + y - 1)(1 - x) - r], \quad (2)$$

$$f_{SD^-}(x, y) = [1 - y + r][(1 - x)(1 - y) + r], \quad (3)$$

$$f_{INT^+}(x, y) = \left[ \frac{1 - y + r}{x(x + y - 1 - r)} \right] [(1 - x)(1 - x - y) + r], \quad (4)$$

$$f_{INT^-}(x, y) = \left[ \frac{1 - y + r}{x(x + y - 1 - r)} \right] [x^2 - (1 - x)(1 - x - y) - r], \quad (5)$$

$$f_T(x, y) = (x + y - 1 - r)(1 + r - y) \quad (6)$$

$$f_{IBT} = \left( 1 + r - \frac{x + y - 1 - r}{x} - \frac{rx}{x + y - 1 - r} \right) \quad (7)$$

$$f_{SDT} = x(1 + r - y) \quad (8)$$

where  $r = \left(\frac{M_\mu}{M_K}\right)^2$  with  $M_\mu$  being the muon mass and

$$A_{SD} = \Gamma_{K\mu^2} \frac{\alpha}{8\pi} \frac{1}{r(1 - r)^2} \left[ \frac{M_K}{F_K} \right]^2, \quad (9)$$

$A_{IB} = 4r\left(\frac{F_K}{M_K}\right)^2 A_{SD}$ ,  $A_{INT} = 4r\left(\frac{F_K}{M_K}\right) A_{SD}$ ,  $A_T = 4A_{SD}$ ,  $A_{SDT} = 4\sqrt{r}A_{SD}$  and  $A_{IBT} = 8\sqrt{r}\left(\frac{F_K}{M_K}\right) A_{SD}$ .

In these formulas  $F_V$  and  $F_A$  are the vector and axial form factors,  $F_T$  is the tensor form factor. We use the prescription [3, 16] for the tensor interaction.  $\alpha$  is the fine structure constant,  $F_K$  is the charged kaon decay constant ( $155.5 \pm 0.2 \pm 0.8 \pm 0.2$  MeV [13]), and  $\Gamma_{K\mu^2}$  is the width of the  $K_{\mu^2}$  decay. As in the paper[19] a minus sign precedes the interference terms, thus changing the sign of the form factors. Without this change in sign the formulas coincide with the ones given in [3, 16].  $SD^+$  and  $SD^-$  refer to the terms with different photon polarizations and do not mutually interfere. Their interference with IB leads to the terms labeled  $INT^+$  and  $INT^-$ . The term SDT refers to  $SD^-T$  interference, the interference with  $SD^+$  is possible only in rather exotic models [4, 5, 6]. The interference between the tensor and inner bremsstrahlung amplitudes is labeled as IBT.

The  $x$  vs  $y$  plots for different terms are illustrated in Figs.1 and 2. The quadrangle area in these figures is restricted by the condition  $x_b < x < x_b + 0.1$  for the  $y$  interval 0.49–1.0, where  $x_b = 1.0 - 0.5(y + \sqrt{y^2 - 4r})$  is the border of the Dalitz plot. This area, characterized by considerable contribution from  $INT^-$ ,  $SD^-$ , IBT and SDT terms, and favourable background conditions is used in our analysis.

Generally form factors can depend on  $q^2 = (p_K - p_\gamma)^2 = M_K^2(1 - x)$ . In our analysis we assume either constant form factors or the phenomenological

dependence for the vector and axial form factors as in [19]:  $F_V(q^2) = F_V(0)/(1 - q^2/M_V^2)$  and  $F_A(q^2) = F_A(0)/(1 - q^2/M_A^2)$  with  $M_V = 0.870$  GeV and  $M_A = 1.270$  GeV. The theoretical situation with  $q^2$  dependence of the form factors is controversial. For  $O(p^4)$  ChPT calculations [1] there is no  $q^2$  dependence,  $O(p^6)$  ChPT calculations [17, 18] predict nearly linear dependence, similar to the phenomenological one. At the same time calculations [17, 18] in the framework of the light-front quark model(LFQM) give quite different dependence with form factors going to zero with  $q^2$  increase.

We assume also the  $q^2$  independence of the tensor form factor  $F_T$ .

The absolute value of the sum of the vector and axial form factors is known with high precision:  $|F_V + F_A| = 0.155 \pm 0.008$ [19], whereas the difference  $F_V - F_A$  is still poorly known. The latest measurement [19] gives for  $F_V - F_A$  only the 90% confidence level:  $-0.04 < F_V - F_A < 0.24$ , whereas the  $O(p^4)$  ChPT prediction is equal to 0.055 [1, 2].

The situation with the tensor contribution is controversial. The measurements have been done mainly for pion decays[8, 9, 10, 11], The observation of the ISTRA experiment[8] was confirmed in the preliminary result by the PIBETA Collaboration[9, 10] having statistically significant deviation from the standard model without tensor term. Latest PIBETA data[11] have however eliminated the evidence for the tensor term and give the limit:  $-0.00052 < F_T < 0.0004$  at the 90% CL. The searches for tensor terms are done also in the studies of the angular distributions in the Gamow-Teller  $\beta$  decays of the spin polarized atoms, see for example [15] and the references therein. These studies are still less restrictive than  $\pi_{e2\gamma}$  data.

It is of interest to note that in some theoretical models [16]  $F_T$  for kaon decay is larger by a factor of  $1/\tan(\theta_C) \sim 4.4$  as compared with pion decay. Here  $\theta_C$  is the Cabibbo angle.

## 2 Experimental setup and event selection

The experiment is performed at the IHEP 70 GeV proton synchrotron U70. The ISTRA+ spectrometer has been described in detail in papers on  $K_{e3}$  [20, 21],  $K_{\mu 3}$  [22, 23] and  $\pi^-\pi^0\pi^0$  decays [24]. Here we recall briefly the characteristics relevant to our analysis. The ISTRA+ setup is located in the negative unseparated secondary beam line 4A of the U70. The beam momentum is  $\sim 25$  GeV/c with  $\Delta p/p \sim 1.5\%$ . The admixture of  $K^-$  in the beam is  $\sim 3\%$ , the beam intensity is  $\sim 3 \cdot 10^6$  per 1.9 sec U70 spill.

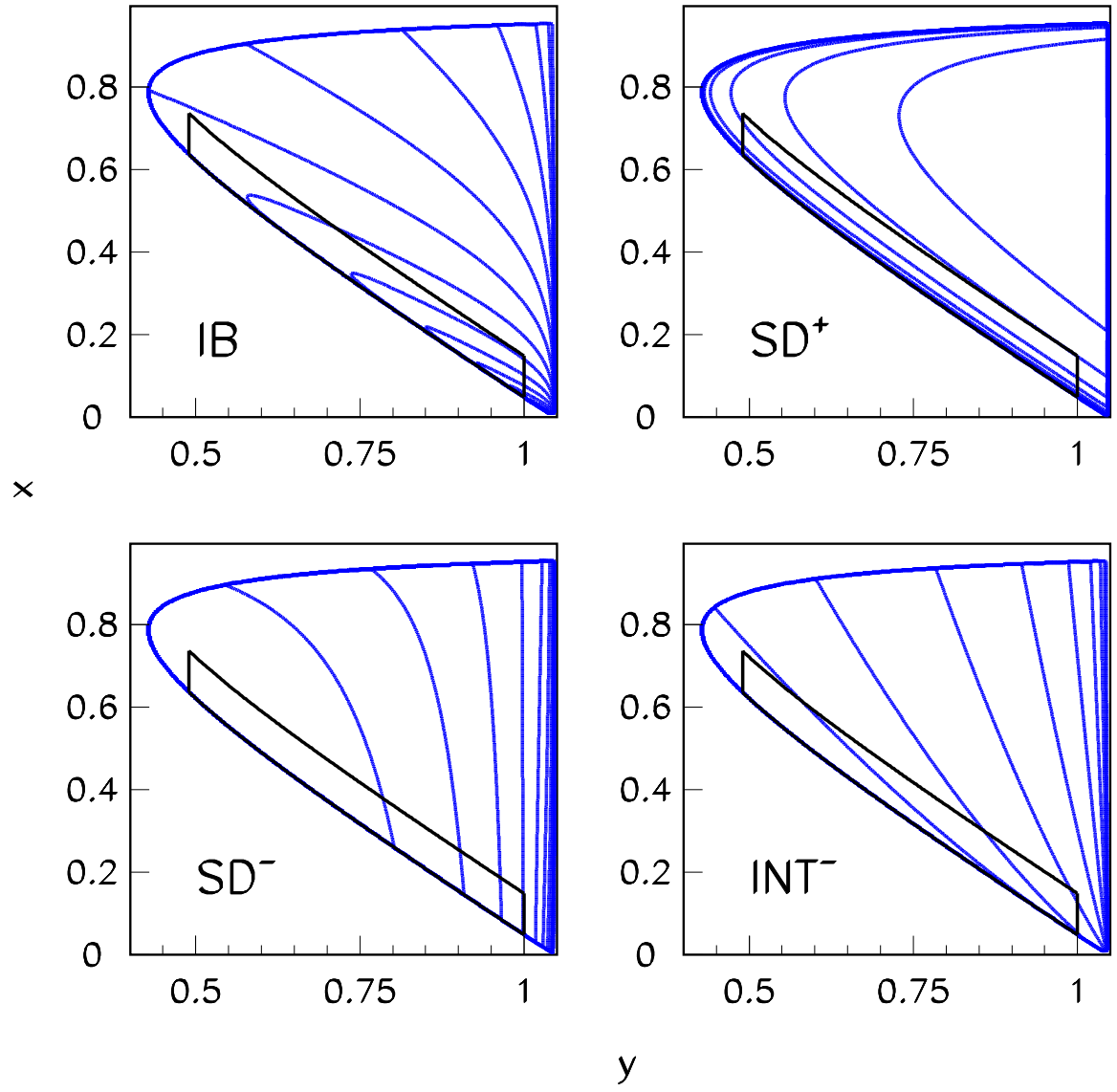


Figure 1: Dalitz plots for IB,  $SD^+$ ,  $SD^-$  and  $INT^-$  contributions. The vertical scale is logarithmic. The quadrangle area shows the region studied.

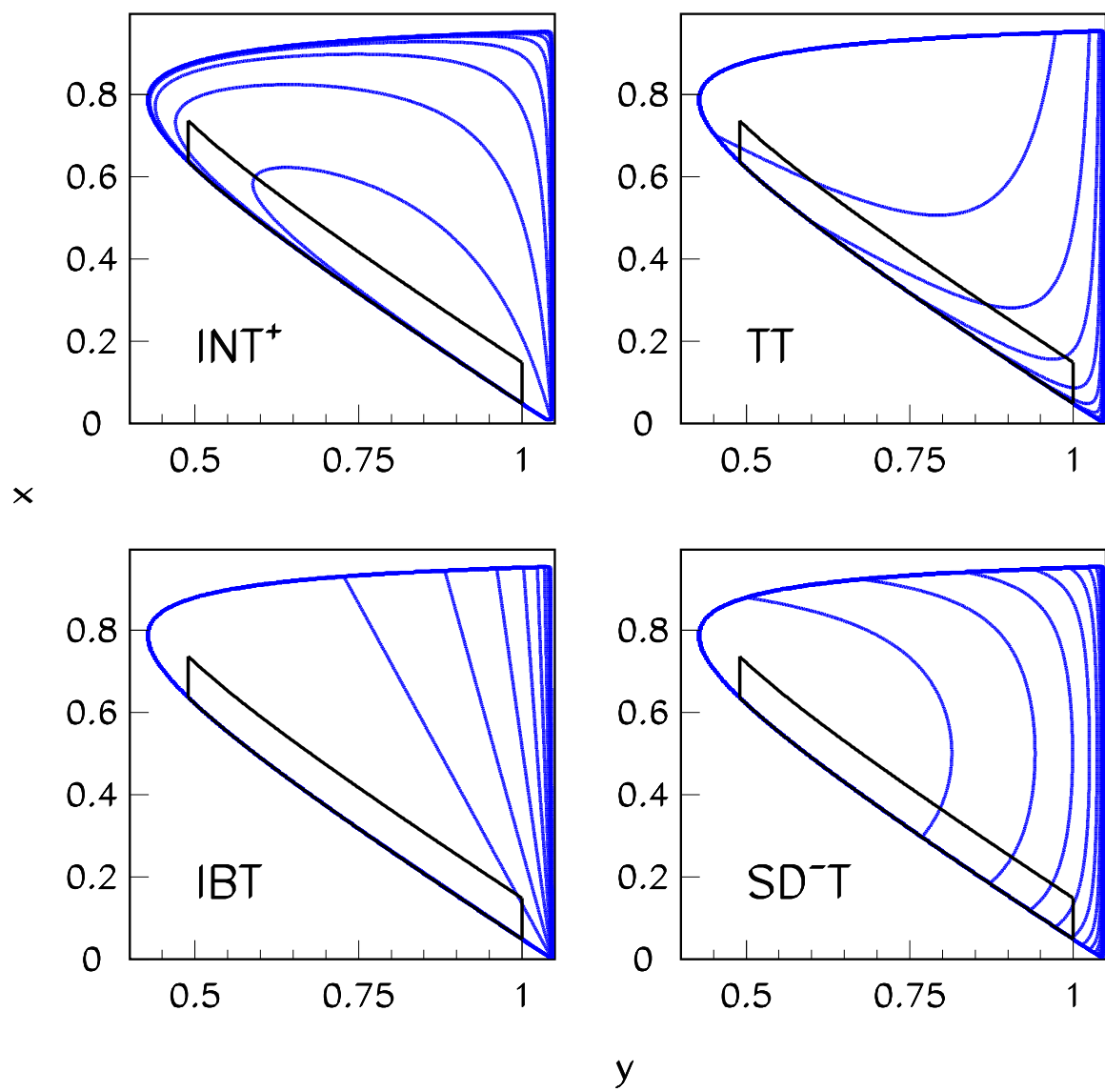


Figure 2: The same as in Fig.1 for  $\text{INT}^+$ ,  $T$ ,  $\text{IBT}$  and  $\text{SD}^-T$  terms.

During the physics run in November-December 2001 350 million trigger events were collected with high beam intensity. This information is complemented by 124 M Monte Carlo (MC) events generated using Geant3 [25] for the dominant  $K^-$  decay modes, 100 M of them are the mixture of the dominant decay modes with the branchings exceeding 1 % and 24 M MC events are the radiative  $K_{\mu 2}$  decays.

Some information on the data processing and reconstruction procedures is given in [20, 21, 22, 23, 24], here we briefly mention the details relevant for present analysis.

The muon identification (see [22, 23]) is based on the information from the electromagnetic calorimeter  $SP_1$  and hadron calorimeter HC. The energy deposition in the  $SP_1$  is required to be compatible with the MIP signal in order to suppress charged pions and electrons. The sum of the signals in the HC cells associated with charged track is required to be compatible with the MIP signal. The muon selection is further enhanced by the requirement that the ratio  $r_3$  of the HC energy in last three layers to the total HC energy exceeds 5 %. The used cut values are the same as in [23].

Events with one reconstructed charged track and one reconstructed shower in the calorimeter  $SP_1$  are selected.

A set of cuts is developed to suppress various backgrounds and/or to do data cleaning:

0) We select events with good charged track having two reconstructed ( $x-z$  and  $y-z$ ) projections and the number of hits in the matrix hodoscope MH below 3.

1) Events with the reconstructed vertex inside the interval  $400 < z < 1600$  cm are selected.

2) The measured missing energy  $E_{mis} = E_{beam} - E_{\mu} - E_{\gamma}$  is required to be above zero.

3) The events with missing momentum pointing to the  $SP_1$  working aperture are selected in order to suppress  $\pi^-\pi^0$  background ( $r > 10$  cm, here  $r$  is the distance between the impact point of the missing momentum and the  $SP_1$  center in the  $SP_1$  transverse plane).

4) We require also the absence of the signal above the threshold in the calorimeter  $SP_2$  and the guard veto system GS.

5) In order to suppress the remaining  $K_{\pi 2}$  contribution at  $y$  around 0.8 we use the cut  $\cos(\phi(\mu\gamma)) > -0.95$  where  $\phi(\mu\gamma)$  is the angle between transverse momenta of the muon and the photon.

We look for the signal in the distributions over the effective mass  $M(\mu^-\gamma\nu)$ ,

where  $\nu$  four-momentum is calculated using the measured missing momentum and assuming  $m_\nu = 0$ . Effective mass spectra for the quadrangular region in Figs. 1 and 2 are shown in Figs. 3,4 and 5 for  $y$ -interval 0.49–1.00 with the step  $\delta y = 0.03$ .

The effective mass spectra have been parametrized by the sum of the signal and of the background. The signal form have been found from the signal Monte Carlo events parametrized by the sum of two Gaussians. The background have been found using the histogram smoothing of the MC background mass spectra by the HQUAD routine from the HBOOK package [26]. This background does not ideally describe the real data, especially at low effective masses. This discrepancy has been taken into account by addition of the term

$$(P(4) + P(5) * M) * \exp(-P(6) * M) \quad (10)$$

to the MC background. It should be noted that the contribution of this term in the signal region is rather small.

First parameter of the fit gives the number of events in the kaon peak, second – the position of the peak, third – normalization of the MC background.

At small  $y$  the signal is rather small, at large  $y$ , especially in the IB region, it dominates over the background. The peak at the effective mass 0.43–0.45 GeV, seen in the histogram o) is the reflection of the remaining  $K_{\pi 2}$  background.

The resulting event distribution in the interval  $0.49 < y < 1.00$  have been parametrized by function constructed using Phase Space signal MC events, weighted with corresponding terms (1)-(8) calculated using “true” MC  $x$  and  $y$  values in the corresponding  $\delta y$  intervals. The results of the fit without tensor component are shown in Fig.6. Here the first parameter is  $F_V + F_A$  fixed at the value 0.155 taken from [19], the second parameter is  $F_V - F_A$ , the third parameter is the tensor form factor and the fourth parameter is the normalization factor. In fact, the fit results are insensitive to the value  $F_V + F_A$  since the  $SD^+$  and  $INT^+$  contributions are negligible, see Fig.6.

The fit is not perfect, but satisfactory,  $\chi^2/\text{NDF} = 34.11/(17 - 2)$  with around three sigma deviation from the expected  $\chi^2$  and  $F_V - F_A = 0.126 \pm 0.027$ .

Several sources of the systematic uncertainty have been studied. The uncertainty given by poor knowledge of the background shape was obtained in two ways. First, by rescaling of the errors in the effective mass distributions in order to have  $\chi^2$  equal to one in each bin and refitting then. Second, by



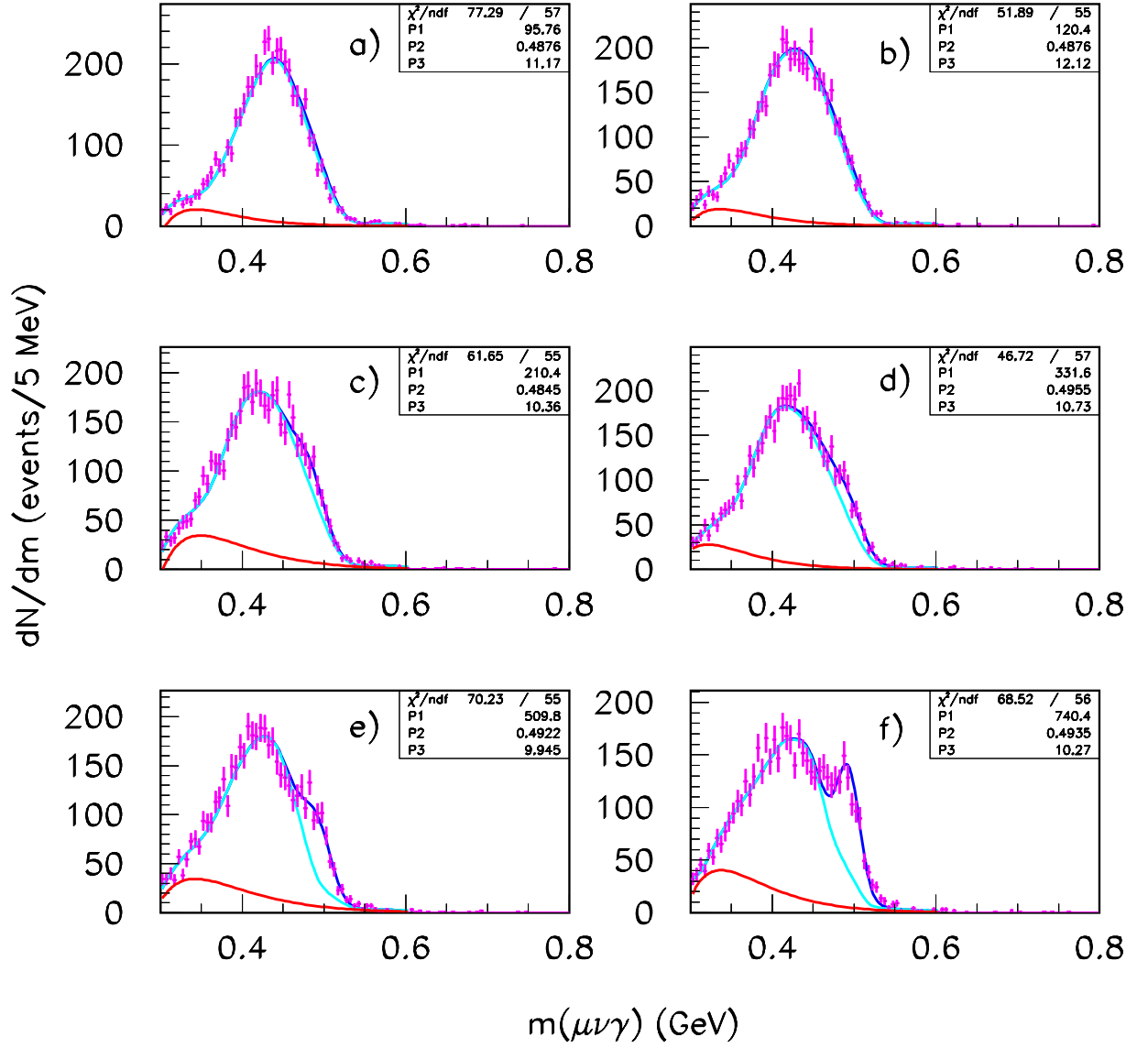


Figure 3: Effective mass  $m(\mu^- \nu \gamma)$  spectra for the  $y$ -interval 0.49–0.67 with the step  $\delta y = 0.03$ .

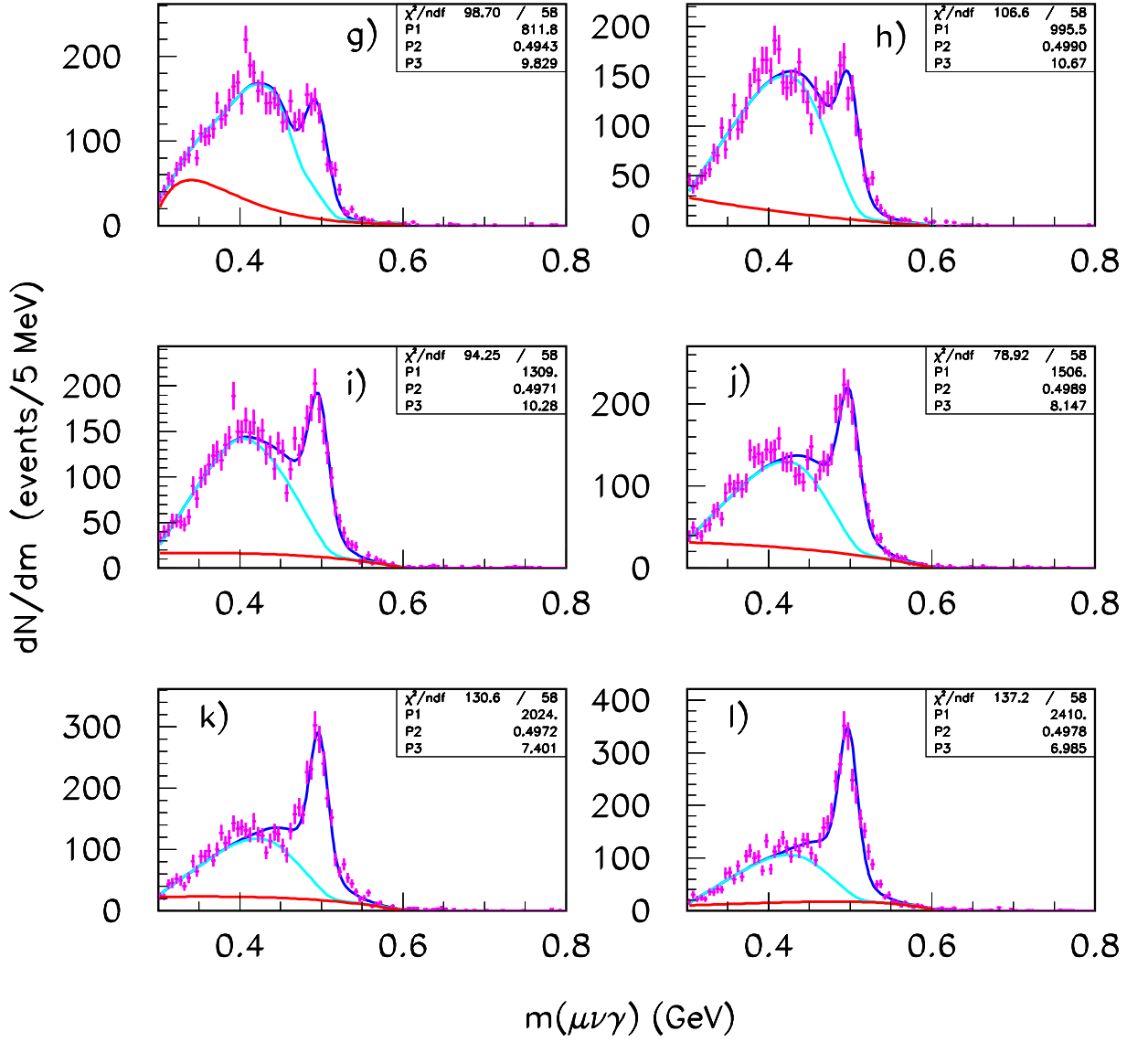


Figure 4: Effective mass  $m(\mu^- \nu \gamma)$  spectra for the  $y$ -interval 0.67–0.85 with the step  $\delta y = 0.03$ .

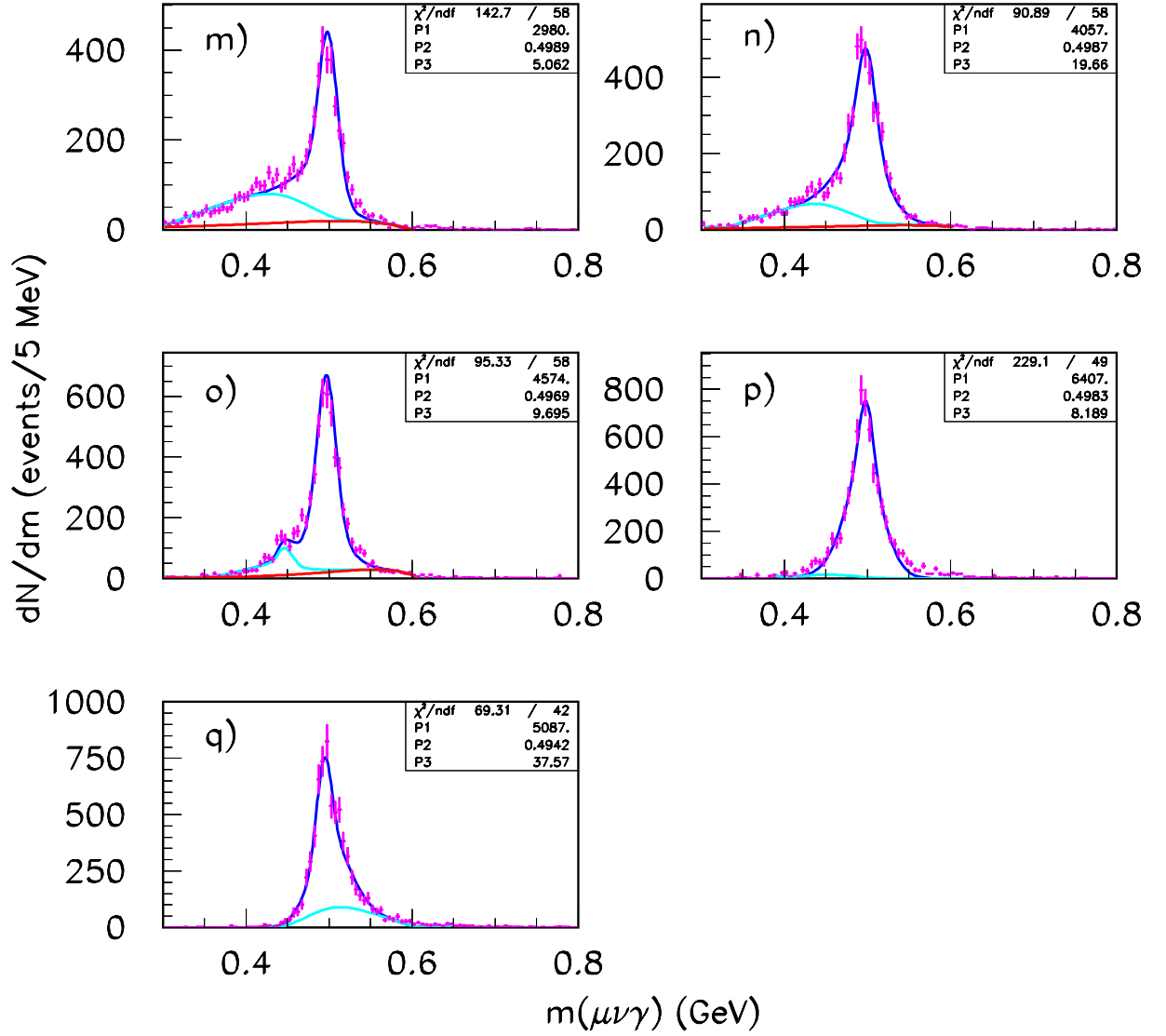


Figure 5: Effective mass  $m(\mu^- \nu \gamma)$  spectra for the  $y$ -interval 0.85-1.00 with the step  $\delta y = 0.03$ .

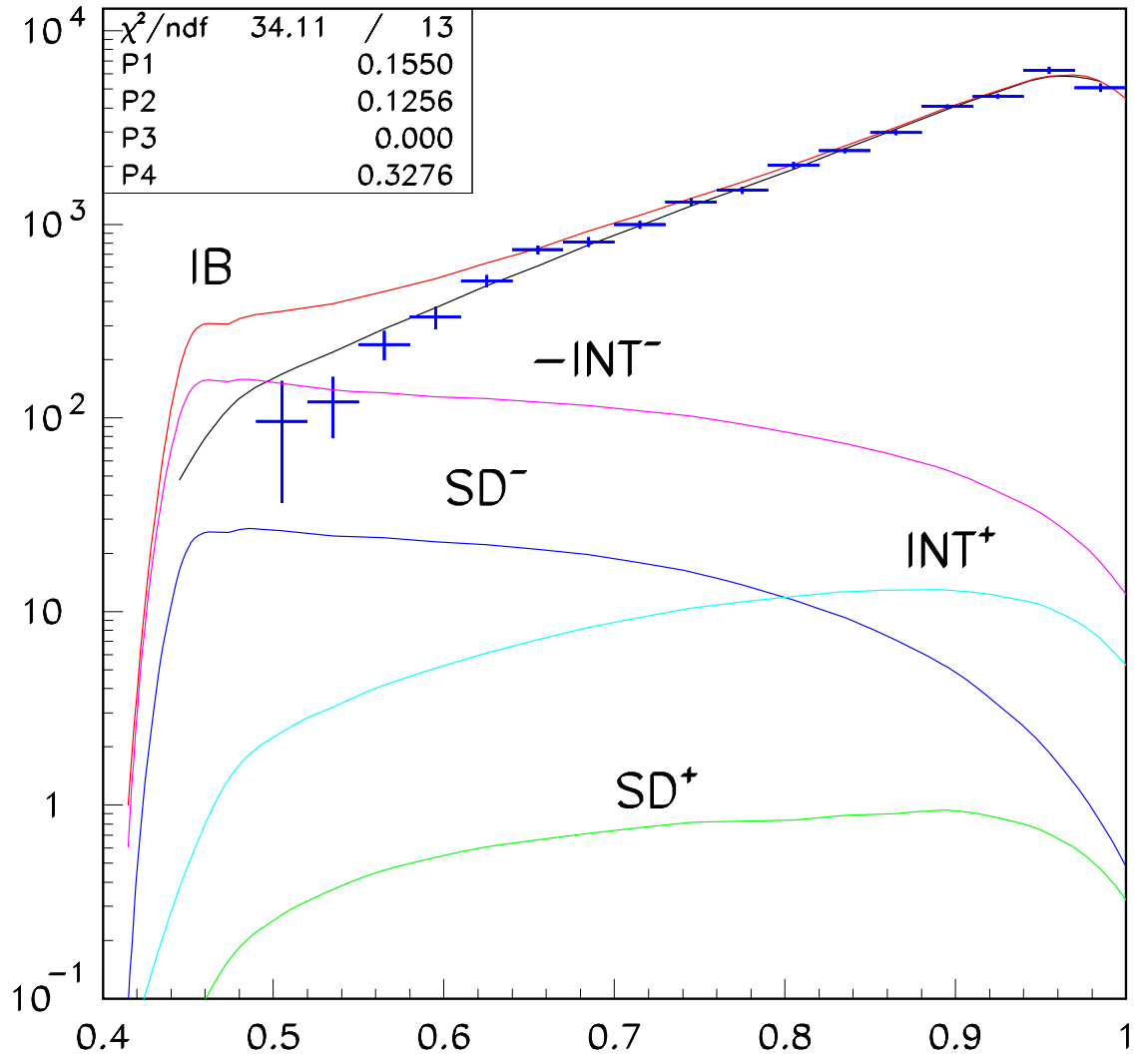


Figure 6: Results of fit of the event distribution with  $F_T = 0$ .

using polynomial parametrization instead of the form (10). First method leads to the deviation in the  $F_V - F_A$  equal to 0.0104, second — to the 0.0086, the maximum of these two values was used as the contribution in the systematic uncertainty. The possible contribution from the  $z$  vertex position was obtained using increased  $z$  interval with maximum  $z$  equal to 1850 cm. This uncertainty is equal to 0.0329. The variation in the muon selection criteria gives the value equal to 0.0167. And the fit in the different  $y$  intervals gives the deviation equal to 0.0191. Adding the individual errors in quadrature we find a total systematic error of 0.0428.

We have tried also the fit with non-zero tensor form factor. The  $\chi^2/\text{NDF}=31.97/(17-3)$ ,  $F_V - F_A = 0.144 \pm 0.044 \pm 0.035$  and  $F_T = -0.0079 \pm 0.011 \pm 0.007$ .

The fit with constant vector and axial form factors gives:  $\chi^2/\text{NDF}=33.4/(17-2)$ ,  $F_V - F_A = 0.146 \pm 0.028 \pm 0.046$  with  $F_T = 0$  and  $\chi^2/\text{NDF}=31.29/(17-3)$ ,  $F_V - F_A = 0.136 \pm 0.060 \pm 0.045$  and  $F_T = 0.006 \pm 0.035 \pm 0.007$ .

### 3 Conclusions

Our conclusions are as follows: The study of the radiative kaon decay  $K_{\mu 2\gamma}^-$  in a new region where  $\text{SD}^-$  and  $\text{INT}^-$  terms have maximum gives the value  $F_V - F_A = 0.126 \pm 0.027(\text{stat}) \pm 0.043(\text{syst})$ . This value is 1.4 standard deviations above  $O(p^4)$  ChPT prediction, equal to 0.055, and probably indicates the need for higher order calculations or for more elaborate analysis of the  $q^2$  dependence of the form factors.

The inclusion of the tensor component gives:  $F_V - F_A = 0.144 \pm 0.044 \pm 0.035$ . and  $F_T = -0.0079 \pm 0.011 \pm 0.007$ , i.e.  $-0.03 < F_T < 0.01$  at 90% CL.

The work is supported in part by the RFBR grant N07-02-00957(IHEP group).

## References

- [1] J. Bijmens, G. Ecker and J. Gasser, Nucl.Phys. B396 (1993) 81.
- [2] see J. Bijmens, G. Ecker and J. Gasser in the “The DAFNE physics handbook”, vol.I, Frascati, 1992.
- [3] E. Gabrielli, Phys.Lett. B301 (1993) 409.
- [4] M.V. Chizhov, Mod.Phys.Lett. A8 (1993) 2753.
- [5] M.V. Chizhov, Phys.Lett. B381 (1996) 359.
- [6] M.V. Chizhov, Phys.Part.Nucl.Lett. 2 (2005) 193.
- [7] P. Herczeg, Phys.Rev. D45 (1994) 247.
- [8] V.N. Bolotov et al., Phys.Lett. B243 (1990) 308.
- [9] D. Pocanic et al., Phys.Rev.Lett. 93 (2004) 181803.
- [10] E. Frlez et al., Phys.Rev.Lett. 93 (2004) 181804.
- [11] M. Bychkov et al., Phys.Rev.Lett. 103 (2009) 051802.
- [12] C. Amsler et al., Particle Data Group, Phys.Lett. B667 (2008) 1.
- [13] J. Rosner and S. Stone, Decay constants of charged pseudoscalar mesons, in [12].
- [14] W. Bertl, Form factors for radiative pion and kaon decays, in [12]
- [15] J.R.A.Pitcairn et al., Phys.Rev. C79 (2009) 015501.
- [16] E. Gabrielli and L. Trentadue, Nucl.Phys. B792 (2008) 48.
- [17] C.Q. Geng, I.L. Ho and T.H. Wu, Nucl.Phys. B684 (2004) 281.
- [18] C.H. Chen, C.Q. Geng and C.C. Lih, Phys.Rev. D77 (2008)014004.
- [19] S.C. Adler et al., E787 Collaboration, Phys.Rev.Lett. 85 (2000) 2256.
- [20] I.V. Ajinenko et al., Phys.Atom.Nucl. 65(2002) 2064; Yad. Fiz. 65(2002)2125.

- [21] O.P. Yushchenko et al., Phys. Lett. B589 (2004) 111.
- [22] I.V. Ajinenko et al., Phys.Atom.Nucl. 66(2003) 105; Yad. Fiz. 66(2003) 107.
- [23] O.P. Yushchenko et al., Phys. Lett. B581 (2004) 31.
- [24] I.V. Ajinenko et al., Phys. Lett. B567 (2003) 159.
- [25] R. Brun et al., CERN-DD/EE/84-1, CERN, Geneva, 1984.
- [26] CN/ASD Group, HBOOK Users Guide(version 4.22), Program Library Y250, CERN, Geneva, 1994;  
J. Allison, Comp.Phys.Comm. 77 (1993) 377.